Production of Purely Spin-Aligned Autoionizing States Which Decay to Orbital-Aligned Ionic States

K. W. McLaughlin, O. Yenen, and D. H. Jaecks
Behlen Laboratory of Physics, University of Nebraska, Lincoln, Nebraska 68588-0111
(Received 2 March 1998)

In violation of the Wigner spin-conservation rule, purely spin-aligned, doubly excited $3p^4[^3P]4p(^2S)$ ns autoionizing states have been produced during the photoionization of argon with linearly polarized radiation. Upon autoionization this spin alignment is transformed into orbital alignment, inferred from the polarized fluorescence from doublet $3p^4 4p$ ionic states. We show that this orbital alignment is equally partitioned between the $3p^4$ subshell and $4p$ valence electron. [S0031-9007(98)06541-7]

PACS numbers: 32.80.Fb

In violation of the Wigner spin-conservation rule [1], we present experimental evidence for the production, by single photon absorption, of purely spin-aligned, doubly excited states of a multielectron system in which the total angular momentum is devoid of orbital content. Excited by linearly polarized radiation, the observed Ar $3p^4[^3P]4p\ ^2S\ ns$ Rydberg states are maximally spin aligned. Upon autoionization this spin alignment is converted into orbital alignment, inferred from the polarized fluorescence from the Ar^+ $3p^4[^3P]4p\ ^2D_{3/2}$ and $^2P_{3/2}$ ionic states. This represents clear experimental evidence for a strong spin-orbit interaction in the decay of an autoionizing state. In addition, we show that this production of orbital alignment in the ionic states is equally partitioned between the $3p^4[^3P]$ subshell and $4p$ valence electron. Thus, our alignment measurements of the $^2D_{3/2}$ and $^2P_{3/2}$ ionic states provide a quantitative measure of the relativistic many-body interaction between the autoionizing ns Rydberg electron with both the $3p^4$ subshell and the $4p$ valence electron.

Excited ionic states produced during photoionization are referred to as satellite states due to their inherent weaker transition rate compared to the main photoline where the residual ion is unexcited. The observation of the fluorescence from these ionic states allows a sensitive study of many-body interactions since measurements can be obtained at threshold with high resolution and efficiency [2,3]. Polarization analysis of this fluorescence, or equivalently, the fluorescence angular distribution, allows one to determine magnetic-substate partial cross sections and the relative strengths of the radial matrix elements for production of photoelectron partial waves [4,5]. In this Letter, we further show that, due to an inferred magnetic sublevel *redistribution,* a measure of a relativistic many-body interaction can be directly quantified from such a polarization analysis.

The satellite states of argon have been observed to display a widely varying angular momentum content, the total angular momentum quantum number varying from $J = \frac{1}{2}$ to as high as $\frac{9}{2}$ [6]. Since the ionizing photon provides only one unit of angular momentum, this implies that there is a significant interaction between the residual atomic electrons and the continuum photoelectron in order to redistribute such an angular momentum content. With no hyperfine structure, and its fine structure resolvable by fluorescence, argon provides a convenient atomic system to explore and quantify the partitioning in such a redistribution. A quantitative measure of this angular momentum sharing can be gleaned from the determination of the total alignment of the excited ionic state since this atomic parameter is one measure of the distribution of the magnetic-substate population [4]. The total alignment parameter can be determined from a measurement of the linear polarization of the fluorescent radiation [7,8].

In the measurements reported here, an atomic beam of argon has been photoionized with synchrotron radiation in the energy range from 35.50 to 35.75 eV with a resolution of 2 to 3 meV. This high resolution without a prohibitive loss of flux was achieved with the spherical-grating monochromator on the 10 cm undulator of beam line 9.0.1 of the Advanced Light Source, Lawrence Berkeley National Laboratory. The linearly polarized synchrotron radiation [9] was made to intersect an effusive beam of argon with the linear polarization axis aligned along the atomic beam axis. Fluorescence was observed orthogonal to this collision plane with a photon-counting photomultiplier coupled to the interaction region by a $f/1.9$ lens along with a linear polarizer and 0.3 nm bandwidth interference filter for fine-structure resolution. By alternating the orientation of the linear polarizer, the fluorescent intensity parallel ($I_\parallel$) and perpendicular ($I_\perp$) to the linear polarization axis of the synchrotron radiation was measured at a fixed ionizing photon energy. Each individual intensity was normalized to the ionizing photon flux monitored by the current on a biased aluminum surface intercepting the synchrotron beam as it exited the interaction region. Repeating the measurement upon incrementing the ionizing photon energy allowed the total intensity $I_t(90°) = I_\parallel + I_\perp$ and linear polarization $P(90°) = (I_\parallel - I_\perp)/I_t(90°)$ of a fine-structure resolved, satellite-state fluorescence spectra to be determined for the polar angle $\theta = (90°)$ with respect to the quantization

axis set by the linear polarization axis of the ionizing radiation. The ionizing energy was incremented by 0.5 or 1 meV sequential steps depending upon the structure observed in exploratory measurements.

Figures 1 and 2 give the total intensity emitted into a 4π solid angle ($= I_{\parallel} + 2I_{\perp}$) and linear polarization $P(90°)$ spectra for the following two Ar^+ $4p \rightarrow 4s$ fluorescent transitions:

$$3p^4[^3P]4p\left\{{}^2D_{3/2} \atop {}^2P_{3/2}\right\} \rightarrow [^3P]4s\left\{{}^2P_{3/2} \atop {}^2P_{1/2}\right\} + \left\{\lambda\ (472.7\ \text{nm}) \atop \lambda\ (476.5\ \text{nm})\right\}.$$

The spectra shown are in the immediate vicinity of the threshold for the excitation of these $4p$ satellite states. As evidenced in Fig. 1, the onsets for these fine-structure resolved thresholds were abrupt with only the dark counts for the photomultiplier tubes registered prior to threshold. The ionizing photon energy was calibrated using the photoelectron yield for the Ar $3s \rightarrow np$ window resonances [10] along with six thresholds for similar satellite state fluorescence [4]. Using microchannel plates, the photoelectron yield was measured along a collection axis lying within the collision plane and aligned at the magic angle with respect to the linear polarization axis of the ionizing radiation. The uncertainties associated with each data point in the figures represent ± 1 standard deviation corresponding to the counting statistics.

Overlain in the figures are predictions for ns and $n'd$ Rydberg series which account for much of the structure in the spectra. Parity and angular momentum conservation restrict the orbital angular momentum of the Rydberg electron to only these values for the indicated excited ionic cores. The series predictions are based on previously accepted [6,10,11] quantum defects for argon along with the well-established [12,13] energy levels for the excited $3p^4[^3P]4p\ ^2P_{3/2}$ and ^2S states of Ar^+.

The autoionizing structure assigned to the $^2P_{3/2}$ ns, $n'd$ series is irregular, most likely due to the interference with early members of the ^2S ns, $n'd$ series as well as the proximity of a comparable ns, $n'd$ series attached to the other fine-structure member $[^3P]4p\ ^2P_{1/2}$ whose energy level is at 35.561 eV. Beyond the limit for $[^3P]4p\ ^2P_{3/2}$ at 35.627 eV, members of the ^2S ns, $n'd$ series show a partially resolved regularity. Although an autoionizing structure has been previously attributed [3] to the $[^3P]4p\ ^2P_{3/2}$ ns, $n'd$ series, the present measurements offer the first experimental evidence for the excitation of the $[^3P]4p\ ^2S$ ns and $n'd$ Rydberg series.

The coupling scheme used to describe the overall symmetry of these doubly excited ^2S $n\ell$ Rydberg states will depend upon the values of n and ℓ [13]; with increasing values of these quantum numbers the coupling proceeds from J_i-ℓ to J_i-j coupling, where J_i denotes the

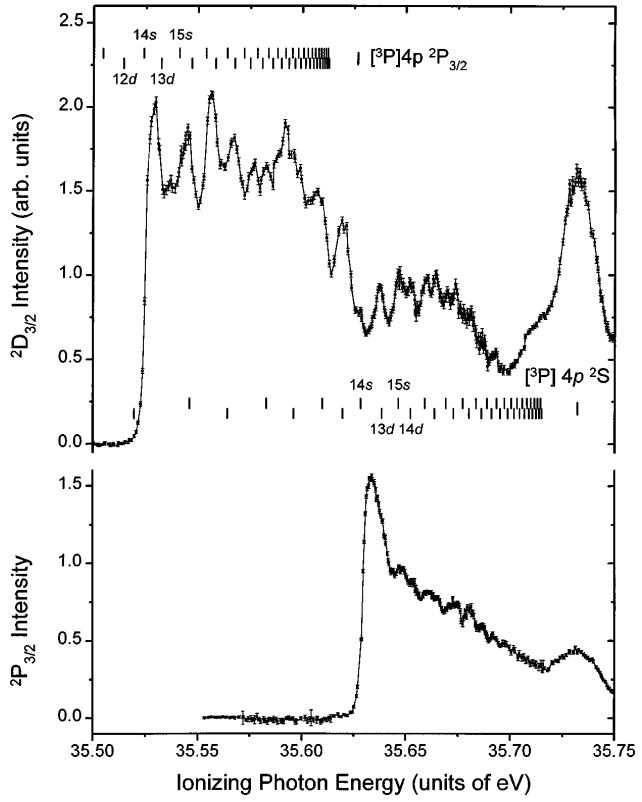

FIG. 1. Total intensity of Ar^+ $3p^4[^3P]4p\ ^2D_{3/2}$ and $^2P_{3/2}$ fluorescence in the immediate vicinity of the thresholds for these satellite states.

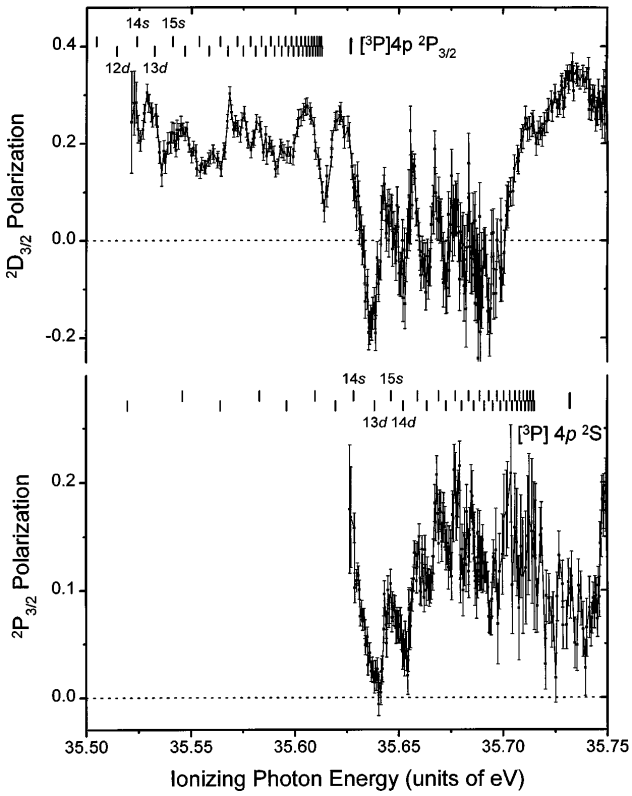

FIG. 2. Linear polarization of Ar^+ $3p^4[^3P]4p\ ^2D_{3/2}$ and $^2P_{3/2}$ fluorescence in the immediate vicinity of the thresholds for these satellite states.

total angular momentum of the ionic core. Independent of the coupling scheme and in apparent violation of the Wigner spin-conservation rule [1], both the $^2S\ ns$ and $n'd$ Rydberg series *require a spin flip during the photoexcitation,* thereby partially explaining the comparable excitation strengths shown in Fig. 1 for both series. In order to satisfy the dipole excitation requirement of a total overall angular momentum of $J = 1$, this spin flip is obvious for the $^2S\ ns$ series and easily illustrated for the $^2S\ n'd$ states from a simple vector model. Thus, the mechanism for the photoexcitation of either of these series is strongly influenced by relativistic spin-dependent interactions. This conclusion is valid to the extent that the $3p^4[^3P]4p\ ^2S$ overall state symmetry is correct, where negligible mixing has been previously assigned [12].

In addition, since these $^2S\ ns$, $n'd$ Rydberg series were excited by a linearly polarized photon, each member of these series must populate the $M_J = 0$ magnetic sublevel only. Thus, in the case of the $^2S\ ns$ series, which is devoid of overall orbital angular momentum, this results in a maximally spin-aligned, doubly excited state. These states are maximally aligned in the sense that the alignment displays an external value and spin aligned in the sense that the total angular momentum is devoid of any orbital content.

Upon autoionization of this $^2S\ ns$ series into the two observed satellite channels, we infer from the observed polarized fluorescence in Fig. 2 that these two satellite states have nonzero alignment [7,8]. Since these satellite states are doublets and, therefore, cannot display any spin alignment, this alignment must reside in their orbital angular momentum. Thus, the spin alignment inherent in the $^2S\ ns$ Rydberg series is transformed into orbital alignment of the satellite states during the decay of this autoionizing series. This represents *clear experimental evidence for a strong spin-orbit interaction in the decay of an autoionizing state.*

During the autoionization

$$3p^4[^3P]4p\ ^2S\ ns, n'd \xrightarrow[autoionization]{} [^3P]4p\begin{Bmatrix} ^2D_{3/2} \\ ^2P_{3/2} \end{Bmatrix} + \varepsilon s, d\,,$$

the $3p^4[^3P]$ subshell does not change its configuration nor its coupling, and the $4p$ valence electron does not undergo a configurational change. The photoelectron kinetic energy results from an overall recoupling between the $3p^4$ subshell and the $4p$ electron. Even though we determine the total alignment parameter [7,8] from our polarization measurement of the satellite state fluorescence, we can *further* quantify the alignment of both the $4p$ valence electron as well as that of the $3p^4$ subshell through an angular momentum decoupling. Thus, our alignment measurements of the $^2D_{3/2}$ and $^2P_{3/2}$ ionic states provide a quantitative measure of the many-body interaction between the autoionizing ns Rydberg electron with the $3p^4$ subshell and the $4p$ valence electron as given by their respective alignment parameters.

Directly proportional to the expectation value of the zero component of the electric quadrupole tensor, the total alignment parameter $A_0(J)$, which is defined [7] as

$$A_0(J) \equiv \frac{\langle 3J_z^2 - J^2 \rangle}{J(J+1)} = \frac{\sum_{M_J} \sigma(J, M_J)[3M_J^2 - J(J+1)]}{J(J+1)\sum_{M_J} \sigma(J, M_J)}, \quad (1)$$

is related to the measured polarization P as follows [8]:

$$A_0(J) = \frac{4P}{h^{(2)}(3 - P)}, \quad (2)$$

where the ionic total angular momentum is now represented as simply J, and $h^{(2)}$ is an angular momentum coupling constant which depends upon the total angular momenta involved in the fluorescence. Figure 3 shows the spectra for the total alignment parameter $A_0(J)$ for the $^2D_{3/2}$ and $^2P_{3/2}$ satellite states determined from the measured linear polarization. There is a positive correlation between the two spectra regarding the structure associated with the $[^3P]4p\ ^2S\ ns, d$ Rydberg series: from the sign of the alignment we can infer that the ns series in both spectra autoionizes to produce a more prolate satellite state charge distribution (in the direction of negative alignment) while the nd series decays to a more oblate distribution (in the direction of positive alignment).

By decoupling the ionic total angular momentum into its constituent angular momentum we can express the

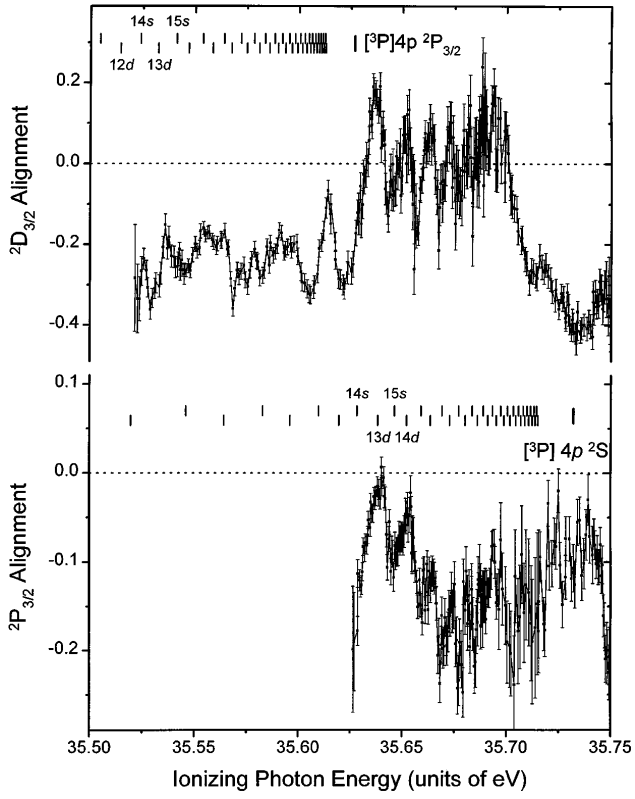

FIG. 3. Alignment of the Ar^+ $3p^4[^3P]4p\ ^2D_{3/2}$ and $^2P_{3/2}$ satellite states in the immediate vicinity of their thresholds.

alignment of the $3p^4$ subshell and that of the $4p$ valence electron in terms of the measured alignment $A_0(J)$. Suppressing state labels unnecessary for the present discussion, let $|J\rangle = \sum_{M_J} a_{M_J}|JM_J\rangle$ represent the superposition of magnetic sublevels composing either of the observed satellite states where the partial cross section $\sigma(J, M_J) = |a_{M_J}|^2 \sum_{M_J'} \sigma(J, M_J')$ contains all of the dynamical information comprising a magnetic substate formation. Decoupling the ionic total angular momentum into its orbital L and spin S components M_L and M_S, respectively [12],

$$|J\rangle = \sum_{M_J} a_{M_J} \sum_{M_L, M_S} \langle LM_L SM_S \,|\, JM_J\rangle \,|LM_L\rangle \,|SM_S\rangle \quad (3)$$

allows the relationship between the partial cross sections for the orbital and total components to be recognized

$$\sigma(L, M_L) = \sum\nolimits_{M_J} \langle LM_L SM_S \,|\, JM_J\rangle^2 \sigma(J, M_L)\,. \quad (4)$$

Substituting (4) into an expression comparable to (1) for the alignment of the orbital angular momentum of the ion yields

$$A_0(L)|_{^2D_{3/2}} = \tfrac{7}{8} A_0(J)|_{^2D_{3/2}} \quad (5)$$

for the relationship between the alignment parameter for the orbital and total angular momentum of the $^2D_{3/2}$ satellite state. The similar relationship for the $^2P_{3/2}$ satellite state is

$$A_0(L')|_{^2P_{3/2}} = \tfrac{5}{8} A_0(J')|_{^2P_{3/2}}. \quad (6)$$

Thus, the alignment parameter for the orbital motion is directly proportional to the measured alignment parameter for the total angular momentum, where the proportionality reflects the purely kinematic, angular momentum coupling constants. The prime designation in (6) is to emphasize that there exists no *a priori* relationship between the alignment parameters for the orbital motion of the two observed satellite states; such a relationship deals with the dynamics represented by the experimental assessment of the total alignment parameter.

This decomposition can be carried one step further by decoupling the total orbital angular momentum of the ion L into its constituent $4p$ electron orbital angular momentum ℓ and orbital angular momentum L_c for the $3p^4[^3P]$ subshell. The L_c-ℓ coupling scheme is an extremely accurate state description for the Ar^+ $[^3P]4p\,^2D_{3/2}$ state which has negligible configuration mixing and is a highly accurate one for the Ar^+ $[^3P]4p\,^2P_{3/2}$ state as well, since this latter symmetry label represents greater than 86% of its state description with mixing of $\approx$13% from the $[^1D]4p\,^2P_{3/2}$ state [12]. The decoupling allows the alignment parameter $A_0(L_c)$ for the orbital motion of the $3p^4[^3P]$ subshell of *each ionic state*, as well as that for the $4p$ valence electron $A_0(\ell)$, to be written in terms of the measured alignment parameters $A_0(J)$ presented in Fig. 3:

$$[A_0(L_c) = A_0(\ell) = \tfrac{1}{2} A_0(L) = \tfrac{7}{16} A_0(L)]|_{[^3P]4p\,^2D_{3/2}} \quad (7)$$

for the $[^3P]4p\,^2D_{3/2}$ state and

$$[A_0(L_c') = A_0(\ell') = -\tfrac{1}{2} A_0(L') = -\tfrac{5}{16} A_0(J')]|_{[^3P]4p\,^2P_{3/2}} \quad (8)$$

for the $[^3P]4p\,^2P_{3/2}$ state. The negative sign in (8) is easily visualized within the vector model of coupling $L_c = 1$ and $\ell = 1$ to yield a composite $L = 1$. The alignment of the composite system will be orthogonal to that of the constituent angular momenta. In both (7) and (8), the development of orbital alignment $A_0(L)$ in the composite system is equally partitioned between the $L_c = 1$ subshell and the $\ell = 1$ electron. This equal partitioning is a necessary physical constraint imposed by the $\mathbf{L} = \mathbf{L}_c + \ell$ coupling appropriate for these states [12]. Thus, the present measurements allow the alignment parameters for the orbital motion of the $3p^4$ subshell and the $4p$ electron to be explicitly quantified. For the doubly excited $3p^4[^3P]4p\,^2S\ ns$ autoionizing states, this orbital alignment originates from an inherent spin alignment. Thus, our alignment measurements of the $3p^4[^3P]4p\,^2D_{3/2}$ and $^2P_{3/2}$ satellite states provide a direct quantitative measure of the relativistic many-body interaction between the autoionizing ns Rydberg electron with both the $3p^4$ subshell and the $4p$ valence electron.

We thank the staff of the Advanced Light Source, Lawrence Berkeley National Laboratory, for their assistance during the acquisition of these measurements and acknowledge the support of the National Science Foundation under Grant No. PHY-9419505.

[1] E. Wigner, Nachr. Akad. Wiss. Geott. Math.-Physik. K1. **IIa**, 375 (1927); J. H. Moore, Jr., Phys. Rev. A **8**, 2359 (1973).
[2] K.-H. Schartner *et al.*, Phys. Scr. **41**, 853 (1990); G. Mentzal *et al.*, J. Phys. B **31**, 227 (1998).
[3] J. A. R. Samson, E.-M. Lee, and Y. Chung, J. Electron Spectrosc. Relat. Phenom. **66**, 75 (1993).
[4] O. Yenen, K. W. McLaughlin, and D. H. Jaecks, Phys. Rev. Lett. **79**, 5222 (1997).
[5] W. Kronast, R. Huster, and W. Mehlhorn, J. Phys. B **17**, L51 (1984); Z. M. Goodman, C. D. Caldwell, and M. G. White, Phys. Rev. Lett. **54**, 1156 (1985); J. Jimenez-Mier, C. D. Caldwell, and D. L. Ederer, Phys. Rev. Lett. **57**, 2260 (1986).
[6] A. A. Wills *et al.*, J. Phys. B **22**, 3217 (1989).
[7] U. Fano and J. H. Macek, Rev. Mod. Phys. **45**, 553 (1973).
[8] B. W. Moudry, O. Yenen, D. H. Jaecks, and J. H. Macek, Phys. Rev. A **54**, 4119 (1996).
[9] N. Berrah *et al.*, J. Phys. B **29**, 5351 (1996).
[10] R. P. Madden, D. L. Ederer, and K. Codling, Phys. Rev. **177**, 136 (1969).
[11] J. A. R. Samson, E.-M. Lee, and Y. Chung, Phys. Scr. **41**, 850 (1990); B. Edlen, in *Handbuch der Physik*, edited by S. Flügge (Springer-Verlag, Berlin, 1964), Vol. 27.
[12] L. Minnhagen, Ark. Fys. **25**, 203 (1963); J. Opt. Soc. Am. **61**, 1257 (1971).
[13] C. E. Moore, *Atomic Energy Levels* (U.S. GPO, Washington, DC, 1971), Vol. I, pp. 211-218.